Daily torpor: When heart and brain go cold —Nonlinear cardiac dynamics in the seasonal heterothermic Djungarian hamster

2009 EPL 88 18002

(http://iopscience.iop.org/0295-5075/88/1/18002)

A Letters Journal Exploring the Frontiers of Physics

October 2009

EPL, **88** (2009) 18002
doi: 10.1209/0295-5075/88/18002

www.epljournal.org

Daily torpor: When heart and brain go cold —Nonlinear cardiac dynamics in the seasonal heterothermic Djungarian hamster

A. Mertens[1], O. Stiedl[2], A. Damm[1] and M. Meyer[1(a)]

[1] *Max Planck Institute for Experimental Medicine - Göttingen, Germany, EU*
[2] *Center for Neurogenomic and Cognitive Research, Vrije Universiteit - Amsterdam, The Netherlands, EU*

received 31 August 2009; accepted in final form 24 September 2009
published online 23 October 2009

PACS 87.18.Nq – Large-scale biological processes and integrative biophysics

Abstract – Djungarian hamsters (*Phodopus sungorus*) acclimated to short photoperiod display episodes of spontaneous daily torpor with metabolic rate depressed by ∼70%, body temperature (T_b) reduced by ∼20 °C, and heart rate (HR) changing from ∼70 bpm during torpor to ∼570 bpm during arousal from torpor associated with remarkable resistance to arrhythmogenesis. The cardiac dynamics of heartbeat interval fluctuations (RR_i) obtained from high-resolution telemetric ECG recordings during daily torpor were studied using nonlinear techniques of signal processing. The nature of cardiac dynamical properties assessed from pointwise Hölder exponents (h) is shifted from strong irregularity of sinus bradyarrhythmia during low-T_b torpor towards smooth regularity on spontaneous rewarming during arousal. The pattern of h fluctuations indicates that both fractality and multifractal properties of RR_i's were decreased during torpor. The cardiac rhythm exhibits both deterministic and stochastic components with intermittency of alterations of prevalence of one over the other on short time scales. During the low-T_b state, RR_i dynamics exhibt nonlinear properties that temporarily shift to linear characteristics during entry into and arousal from torpor. Sympatho-vagal antagonism of autonomic cardiac control is markedly relaxed but remains active and highly alert when animals are torpid and temporarily out of the mainstream of competition.

Introduction. – The maintenance of a constant high body temperature (T_b) in small body-sized euthermic mammals over a wide range of fluctuating ambient temperatures (T_a) is energetically expensive. In order to escape from unfavorable climate conditions and/or limited food supply, many small mammals have retained strategies to minimize their energy expenditure by entering states of deep hibernation in true hibernators or shallow daily torpor in daily heterotherms during which metabolic rate ($\dot{M}$), T_b, and other physiological variables are substantially reduced (for reviews, see [1–8]).

Remarkably, the Djungarian or Siberian hamster (*Phodopus sungorus*) which inhabits high-latitude regions of Siberia and China opportunistically undergoes episodes of daily torpor for ∼5–10 h with T_b as low as 19 °C. Notably, unlike in homeothermic mammals, cardiac contractility is preserved during low T_b and the myocardium is also resitant to the induction of conduction block or tachyarrhythmia during entrance into torpor which is a relatively slow process or during arousal which is rapid and completed within ∼2 h.

The understanding of the cardiac function during the heterothermic daily torpor has remained incomplete [9,10]. A contested issue relates to the degree to which the autonomic nervous system (ANS), in particular its role in determining the cardiac rhythm, is effective during hibernation or daily torpor and arousal from these states [10–14]. The components of the ANS cannot be investigated directly *in vivo*. However, the output of integrated, multiple-component physiologic systems under neuroautonomic regulation, such as HR, exhibits complex nonequilibrium homeodynamic fluctuations that, even in resting conditions and in the absence of external perturbations, go beyond the traditional concept of homeostatic equilibrium dynamics [15–22]. The dynamical properties of HR can be associated with well-known mechanisms of neuroautonomic control, *i.e.*, sympatho-vagal antagonism. Hence, the dynamical beat-to-beat fluctuations represent an operational "window" on brain-heart interactions, the variability in the cardiac time series reflecting the collective efferent traffic of the ANS associated

(a) E-mail: meyer@em.mpg.de

with the individual's state during intrinsic or extrinsic challenge.

In this study, the dynamical properties of cardiac adjustment were analyzed in Djungarian hamsters during entrance into torpor, in deep torpor, and during arousal. The dynamics of the cardiac rhythm, *i.e.*, the time series formed by the time increments between consecutive heart beats (RR_i), was assessed by nonlinear measures of irregularity/regularity (pointwise Hölder exponents, h) and evaluated for deterministic/stochastic and nonlinear/linear properties (Delay-Vector Variance analysis) using randomized and linearized surrogate data. An important finding was that, in the heterothermic state of torpor ($T_b \sim 21\,^\circ$C), HR ($\sim$70 bpm) is lowered to $\sim$20% of its euthermic level ($\sim$350 bpm) and displays marked sinus bradyarrhythmia (increasing amplitude of RR_i fluctuations). The appearance of enhanced irregularity yielding a "noisy" and highly "erratic" or potentially "random" pattern of the cardiac rhythm is intriguing as randomness in the strict mathematical understanding is not an inherent ontological property of nature.

Methods. – Below, we will heuristically introduce the nonlinear techniques of data processing; experimental techniques and additional mathematical details are given in online Supplemental Information (SI) at `http://www1.em.mpg.de/meyer`.

Wavelet Multiresolution Analysis (WMRA). The wavelet-based multiresolution analysis of a time series yields a detailed survey of the fluctuations on a scale-by-scale basis. The Maximal Overlap Discrete Wavelet Transform (MODWT) provides for a scale-based additive decomposition of the time series with zero phase output. The smooth $S_6(n)$ which captures the trend of the RR_i fluctuations at a scale of $2^6 = 64$ consecutive heartbeats provides a reasonable estimate of the baseline drift (RR_B) or trend in the RR_i time series (see SI).

Pointwise Hölder regularity. The RR_i time series presents a signal that is a non differentiable singular function at almost all points in time. A singularity occurs when RR_i undergoes abrupt changes. In nonlinear analysis of highly irregular time series, the strength of a singularity, indicating the local regularity/irregularity of the RR_i signal, is characterized by its pointwise Hölder exponents (h) with dimensionless values defined in a compact of [0,1]. The Hölder exponents designate the local smoothness of the time series, the smaller h, the more irregular the function (see SI).

Surrogate data. The identification of deterministic/stochastic and/or nonlinear/linear dynamics within a signal is important towards understanding complex system behavior because both deterministic and stochastic as well as nonlinear and linear dynamics often coexist in the same system. Statistical analysis by the concept of "surrogate data" tests for a difference between a "test statistic" computed for randomly permutated or linearized versions of the data, *i.e.*, an ensemble of realizations of the null hypothesis of random or linear dynamics. First, a residual probability α of a false rejection is selected, corresponding to a level of significance $(1-\alpha)\times 100\%$. Next, $M = K/\alpha - 1$ randomly permutated or linearized sequences are generated with $K = 2$ (two-tailed test). Thus, for a nonparametric rank-order test at the 95% level of significance ($\alpha = 0.05$), a collection of $2/\alpha - 1 = 39$ surrogates is required (see SI).

Delay-Vector Variance (DVV). The delay-vector variance analysis is based on the calculation of the "target variance", σ^{*2}, of a time series that is embedded in the so-called state-space which serves to reconstruct a facsimile of the phase-space dynamics of some multidimensional system from the observation of a single variable. The minimal target variance, σ^{*2}_{min}, is inversely related to prevalence of the deterministic component over the stochastic one, lowest σ^{*2}_{min} indicating the strongest determinism. For identification of the random or linear nature of an experimental time series, the DVV analysis is expanded for multiple randomized and linearized surrogate time series realizations (see SI).

Results. – In the strictly photic-entrained Djungarian hamster, spontaneous daily torpor occurs at predictable times of the day. This species exhibits a robust rhythm typical of a nocturnal species and T_b drops by $\sim$20 °C during episodes of lethargy.

Pattern of heart rate during torpor. The time course of RR_i and T_b during entrance into and arousal from daily torpor is shown in fig. 1 for all animals in study. The increasing amplitude of the RR_i fluctuations is a reflection of sinus bradyarrhythmia during progression of depth of torpor which is rapidly reversed upon arousal. In order to recover the "baseline" trend of the signal that is embedded in the "noise", the property of Wavelet Multiresolution Analysis (WMRA) by Maximal Overlap Discrete Wavelet Transform (MODWT) to fully decompose a signal on a hierarchy of details and a smooth part suggests to selectively eliminate fast fluctuations in the original (*denoising*). The extracted baseline trend (RR_B) is included in fig. 1 (red lines). While the amplitude of the RR_i fluctuations is markedly enhanced and the "baseline" of the RR_i intervals prolonged (bradycardia), the residual fluctuations of RR_B reveal that the original time series is *nonstationary*. The nonstationarity of RR_i in unrestrained torpid hamsters presents an intrinsic property of RR_i dynamics and would not result from external factors such as varying degrees of physical activity because hamsters remain in a *sleep-like resting condition* throughout the torpor cycle. We also note, that the arrhythmia in all animals (fig. 1) was strictly that of sinus bradycardia, because analysis of ECG morphology revealed that every P-wave was followed by a QRS-complex (see SI, fig. 7). The ECG morphology and myocardial conduction properties in Djungarian hamsters have recently been analyzed in detail [23]. In euthermia, T_b was $36.7 \pm 0.5\,^\circ$C, decreasing at a rate of $3.2 \pm 0.8\,^\circ$C/h, reaching its minimum at $21.0 \pm 2.0\,^\circ$C within 7.8 ± 1.0 h after onset of torpor. During arousal, T_b increased at a maximum rate of $22.5 \pm 4.3\,^\circ$C/h and

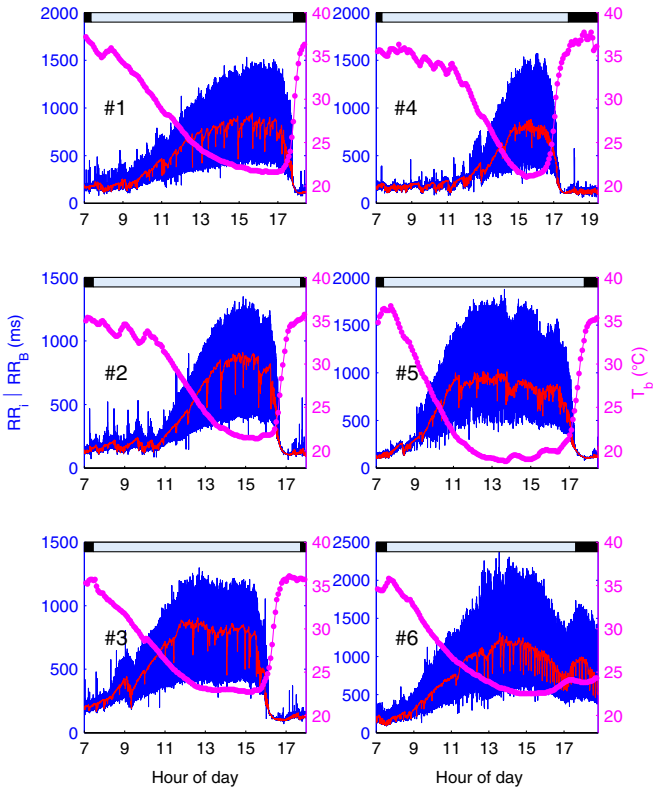

Fig. 1: Daily torpor in *P. sungorus* ($n = 6$). Instantaneous (RR_i, blue) and baseline (RR_B, red) interbeat intervals (left axes) and body temperature (T_b, magenta, right axes). Sunrise and sunset are indicated by the horizontal bars.

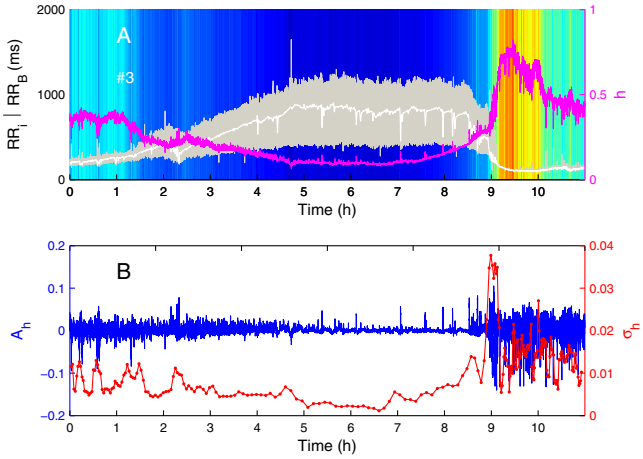

Fig. 2: Regularity of RR_i dynamics during daily torpor. A) Instantaneous (RR_i, grey) and baseline (RR_B, white) interbeat intervals (left axis) and Hölder regularity (h, magenta, right axis). The irregularity of h is also represented as a colored "barcode" where the range of colors shows the range of local irregularity and the distribution of the colors (blue = irregular; red = smooth) within the RR_i series illustrates the distribution in time of the local irregularities. B) Amplitude fluctuations of h (A_h, blue, left axis) and SD (σ_h, red, right axis) calculated from 2048-points segments with 512-points offset.

recovery to euthermic T_b was completed within ∼40 min. Hamsters did not become physically active immediately after arousal but remained in a sleep-like "posttorpor inactivity state" characterized by lack of locomotion or feeding activity.

At euthermia, RR_B was ∼175 ms (≈343 bpm), increasing (decreasing) to maximum (minimum) levels of ∼860 ms (≈70 bpm) during torpor. Animals displayed a sustained tachycardia in the early "posttorpor inactivity state" (RR_B ∼105 ms, ≈570 bpm) that did not revert to pretorpor levels for up to 2 h. While the RR_i amplitudes are substantially increased upon progression of depth of torpor, they rapidly decline on arousal and the variability of RR_i is at its minimum in the early "posttorpor inactivity state". The time course of RR_B, unlike that of T_b, is far from being smooth contiguously throughout the torpor bout but displays intermittency by interspersion of short-term (from ∼3 to ∼4.5 min) episodes of cardioacceleration. Remarkably, the "chronotropic competence" of the myocardium over an 8-fold dynamical range of HR is well preserved which highlights the resistance of myocardial excitation/conduction patterns to evolution of arrhythmogenesis when T_b is changing by ∼20 °C within ⩽1 h during arousal.

Hölder regularity. The pointwise Hölder exponent (h) of a function (or time series) is a local roughness characteristic calculated at every point where the function is defined. The rapid changes in the time series are called *singularities* of the signal and their strength is measured by h. It reflects a local power law, *i.e.*, the decay rate of the amplitude of the function's fluctuation in the neighborhood of that point as the size of the neighborhood shrinks to zero. Highly irregular points in a function are characterized by lower values of h and a smoother portion has higher values of h. When h changes across the time series due to variation in the local noninteger fractal dimension ($D = 2 - h$ [24]), the underlying process is a member of a special class of complex processes referred to as multifractals. The values of h strictly stay within the unit interval [0,1] which indicates fractality and implies that the function is not differentiable anywhere [25]. Different values of h indicate different degrees of fractality.

The temporal structure of local h for a typical torpor bout is shown in fig. 2A. During entrance into torpor h is decreased from ∼0.38 to ∼0.1, indicating that the roughness of the RR_i series is markedly enhanced as a result of sinus bradyarrhythmia. Further on, h shows a sluggish increase prior to any changes of T_b or RR_B and rapidly, within ⩽1 h, increases to ∼0.8 during arousal, *i.e.*, RR_i dynamics are shifted from strong irregularity towards smoother regularity. The profile of h indicates that D of the cardiac RR_i's monotonically increases with depth of torpor, while the reversal takes on during arousal. The amplitude of the fluctuations of h (A_h, quantified by SD, σ_h; calculated for overlapping segments, $N =$ 2048, 512-points offset) which gives an estimate of the

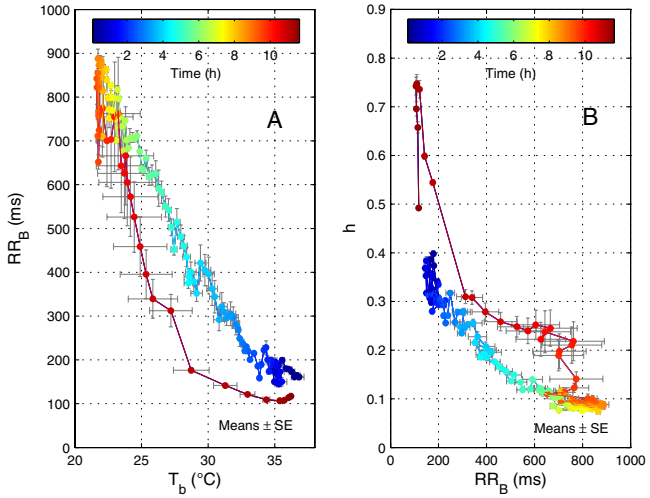

Fig. 3: RR_B *vs.* T_b (A) and h *vs.* RR_B during daily torpor (B). Bidirectional group means ± SE, color-coded according to length of the torpor cycle.

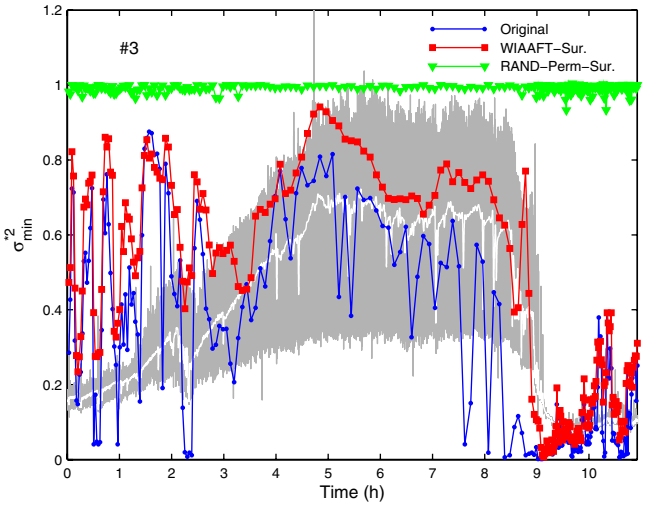

Fig. 4: Determinism and stochasticity of RR_i during daily torpor. Minimum target variance (σ^{*2}_{min}) from DVV analysis for original RR_i series (blue) and for WIAAFT (red) and RAND-PERM (green) surrogates. RR_i (grey) and RR_B (white) in background are displayed for orientation.

inhomogeneity of multifractal properties is decreased and implies that multifractality is decreased with progression of torpor depth (fig. 2B, see SI). Lower h associated with lower σ_h indicates that both fractality and multifractality were decreased. The results suggest that the mechanisms driving RR_i variability during a torpor bout go through various levels of multifractality.

Temperature, heart rate and regularity. The RR_B/T_b relationship throughout the torpor cycles is shown in fig. 3A for all individuals. Group means ± SE were obtained by spline interpolation for adjustment of individual RR_B/T_b data to equal data lengths and bidirectional averaging. RR_B increased with decreasing T_b in an almost linear fashion ($\Delta RR_B \sim 55\,\mathrm{ms}/^\circ\mathrm{C}$), indicating that RR_B was a close function of downregulation of $\dot{M}$ and the ensuing fall of T_b, consequent upon lack of heat production. By contrast, T_b lagged RR_B during arousal yielding a hysteretic loop of the RR_B/T_b relationship resulting from sluggish loading of tissue heat capacitances which is characteristic for all mammals arousing from hibernation or daily torpor.

The h/RR_B relationship is displayed in fig. 3B. During progression of torpor, h is decreased from ~ 0.38, approaching $\sim$0.09 prior to onset of arousal. On arousal, h rapidly increases and follows a counter-clock wise hysteretic loop. Thus, for the same RR_B, *e.g.*, 600 ms, the regularity of RR_i dynamics is substantially different as a result of whether the animal enters into low-T_b torpor or rewarms during arousal. However, while the RR_B/T_b hysteresis results from a physical capacitance effect of the rate of change of endothermic heat production, *i.e.*, the kinetics of accumulating heat charge or heat dissipation of tissues, the h/RR_B hysteresis is a reflection of "active" control of cardiac dynamics. The results suggest that HR, which is linked to $\dot{M}$, is the variable under "active" control while concomitant T_b reflects the dependent variable that is associated with $\dot{M}$ depression (torpor) or activation (arousal). Here, we emphasize that the hysteresis of the RR_B/T_b and h/RR_B relationships reflect nonlinear phenomenona which strictly imply that the mechanisms underlying entry into and arousal from torpor are substantially asymmetric and different from each other.

Determinism and stochasticity. In the following, we restrict to the "typical" RR_i pattern of *animal 3*. The findings may be generalized as the results were quantitatively similar for all animals shown in fig. 1. The minimum target variance (σ^{*2}_{min}) obtained from DVV analysis (calculated for overlapping RR_i segments, $N = 2048$, 512-points offset) throughout a torpor cycle is shown in fig. 4. σ^{*2}_{min} shows wide fluctuations between strong determinism (small σ^{*2}_{min}) and strong stochasticity (large σ^{*2}_{min}) where intermittency of marked determinism is associated with short-term episodes of cardioacceleration. Maximum stochasticity (high σ^{*2}_{min}) is approached about half-way of the heterothermic state gently relaxing in the 2nd half prior to the onset of arousal. Throughout arousal and during the "posttorpor inactivity state" the nature of the RR_i dynamics is strongly deterministic. The $\bar{\sigma}^{*2}_{min}$ means of 39 *randomized* surrogates (RAND-PERM) of the original RR_i segments, *i.e.*, realizations of the null hypothesis of strict randomness, scatter around their theoretical values ($\sigma^{*2}_{min} = 1.0$). The distance between σ^{*2}_{min} of the original RR_i segments and its randomized reference indicates that the irregularity of RR_i dynamics during torpor is close to random dynamics but would not conform to randomness (white Gaussian noise) in the strict mathematical sense. It appears that one of the

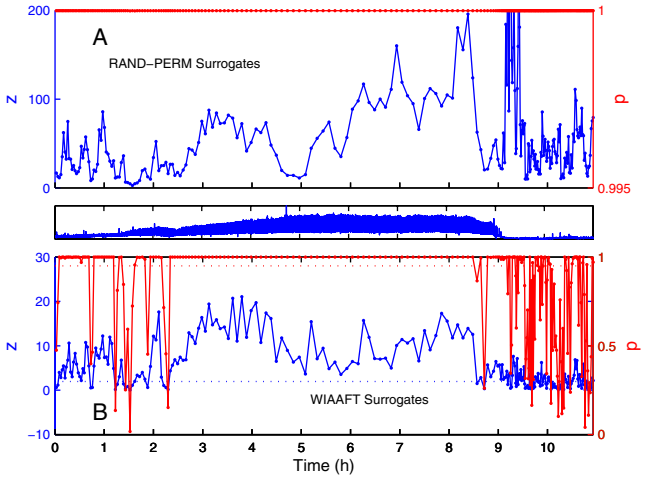

Fig. 5: Randomness and nonlinearity of RR_i during daily torpor. A) z-scores of randomized (RAND-PERM) surrogates (blue, left axis) and probability p (red, right axis). B) z-scores of linearized (WIAAFT) surrogates. Dotted lines refer to $z = 1.96$ and $p = 0.95$, respectively. RR_i time series is shown in middle panel for orientation.

basic tenets of cardiac control is to drive RR_i fluctuations away from the limiting state of (uncontrolled) randomness which is incompatible with life. Similarly, $\bar{\sigma}^{*2}_{min}$ means of 39 *linearized* surrogates (WIAAFT), *i.e.*, realizations of the null hypothesis of linearity, are, for the most part, larger than σ^{*2}_{min} of the corresponding original RR_i segments, indicating that the RR_i dynamics exhibit a nonlinear component which, in concert with strong determinism, disappears upon arousal and during the "posttorpor inactivity state".

Randomness and nonlinearity. Statistical testing using randomized (RAND-PERM) and linearized (WIAAFT) surrogates of RR_i segments is compiled in fig. 5. Throughout, the two-sided z-score is > 1.96 and the probability $p > 0.95$, suggesting that the null hypothesis of strict randomness may safely be rejected (fig. 5A). The distance of z from 1.96 designates the "magnitude" of deviation from the null hypothesis of randomness. Along these lines, statistical testing using linearized surrogates reveals the occurrence of linear RR_i segments ($z < 1.96$, $p < 0.95$) early during entry into torpor and after arousal while RR_i's during deep torpor consistently exhibit nonlinear dynamics (fig. 5B).

Discussion. – This study presents a comprehensive analysis of RR_i fluctuations in a species that resorts to the strategy of daily torpor as a metabolic saving. Physiological signals, such as the RR_i time series of hamsters undergoing daily torpor, are typically generated by complex self-regulatory systems that process inputs with a broad range of characteristics. Such physiological time series fluctuate in an irregular and complex manner and the statistics often exhibit self-affine or fractal properties. The analysis demonstrates that the irregular fluctuations of RR_i's display more intrinsic structure than can be captured by traditional methods. The nonparametric methods of analysis are attractive, because they do not *a priori* assume any mathematical structure (*e.g.*, stationarity or linearity). Physiological time series may be visualized as "badly behaved" data originating from instabilities driven by the intrinsic nonlinear correlated dynamics of a (multi)fractal process. A fractal process typically produces a time series with long-run dependence of the fluctuations that display a "drift-like" appearance at all time scales. In contrast, a random process cannot produce dynamical evolution or structure, as this would contradict the second law of thermodynamics. It has been shown previously that multifractal cardiac dynamics in humans and mice were generated by neuroautonomic mechanisms rather than by extrinsic behavior-dependent modifiers [15–22].

The present analysis demonstrates that the nature of RR_i intervals in *Phodopus* is neither strictly deterministic nor strictly random and cardiac control acts to keep cardiac dynamics well within the range bounded by these extremes. The DVV analysis, using the decisive measure of σ^{*2}_{min} (fig. 4), has delineated that the random-like RR_i dynamics exhibit both deterministic *and* stochastic components. Intermittent alteration of prevalence of the deterministic over the stochastic one designates the persistence of "active" cardiac control throughout the torpor cycle. Active control is manifested in short-term episodes of cardioacceleration that is recovered in the MODWT-denoised RR_B series (figs. 1, 2, 4). During torpor, the degree of stochasticity and nonlinearity is markedly enhanced which is also reflected in the increased fractal dimension (D) *viz.* decreased Hölder regularity (h). The expression of more stochastic components during dormancy is associated with a decreasing level of multifractality, both findings may be taken as signature of increased instability *viz.* decreased complexity of RR_i dynamics and its underlying mechanisms. The neuroautonomic regulation of RR_i dynamics has previously been modeled by the concept of "stochastic feedback" [26].

There is no agreed-on definition of the term complexity which is typically defined operationally by its measure. Notably, strictly random dynamics would exhibit highest complexity because of its high information density and the inability to predict its future evolution. However, the underlying mechanisms are just trivial (by chance) and not really complex. The analysis demonstrates that the complexity of RR_i dynamics, decreasing during torpor, is continually changing throughout the dormant state but the most prominent alterations are observed during the initial state of entry into torpor and upon arousal. For most of the dormant state, RR_i dynamics exhibit nonlinear properties but operation of strongly deterministic control mechanisms during arousal and throughout the "posttorpor inactivity state", driving RR_i's into sustained tachycardia, leads to temporary changeover into linear dynamics. The *instability* of dynamical properties may

be associated with the behavior of dynamical systems operating *far away from equilibrium* [17,20,26]. In that regard, cardiac control is operating over a wide range of nonequilibrium regimes, eventually approaching near to equilibrium, as its basic tenets appears to effectively drive the system away from strict determinism or strict randomness.

The dynamical properties of RR_i time series can be associated with well-known mechanisms of cardiac control mediated by the efferent SNS and PNS branches of the ANS. In general, SNS and PNS nerve activities operate reciprocally: *sympatho-vagal antagonism*. During sojourn into torpor, sympatho-vagal antagonism is expected to be relaxed, mainly in proportion to decreasing T_b, which, in dynamical terms, is expressed by decreasing levels of multifractility (fig. 2). However, ANS activity, presumably being markedly reduced, is not simply arrested but remains functionally operative throughout the full-length torpor cycle. Ongoing control of heart by the ANS is reflected in the time course of Hölder regularity (h), by intermittency of alterations of prevalence of deterministic/stochastic dynamics on short time scales, and short-term readjustment of multifractal properties of cardiac dynamics. The dramatic changes during arousal and throughout the "posttorpor inactivity state" may be associated with SNS (hyper)excitation and absence of concurrent PNS recruitment. Notably, brain-heart signaling *via* ANS mechanisms during onset of arousal, *i.e.*, when T_b is still low, leads support to the concept that ANS control of heart is well preserved in the heterothermic state of torpidity.

REFERENCES

[1] Boyer B. B. and Barnes B. M., *Bioscience*, **49** (1999) 713.
[2] Carey H. V., Andrews M. T. and Martin S. L., *Physiol. Rev.*, **83** (2003) 1153.
[3] Geiser F., *Annu. Rev. Physiol.*, **66** (2004) 239.
[4] Heldmaier G. and Klingenspor M., *Life in the Cold* (Springer, Berlin) 2000.
[5] Heller H. C. and Ruby N. F., *Annu. Rev. Physiol.*, **66** (2004) 275.
[6] Lyman C. P., Willis J. S., Malan A. and Wang L. C. H., *Hibernation and Torpor in Mammals and Birds* (Academic, New York) 1982.
[7] Ruby F. N., *J. Biol. Rhythms*, **18** (2003) 275.
[8] Körtner G. and Geiser F., *Chronobiol. Int.*, **17** (2000) 103.
[9] Harris M. B. and Milsom W. K., *J. Exp. Biol.*, **198** (1995) 931.
[10] Milsom W. K., Zimmer M. B. and Harris M. B., *Comp. Biochem. Physiol. A*, **124** (1999) 383.
[11] Twente J. W. and Twente J. A., *Autonomic regulation of hibernation by Citellus and Eptesicus,* in *Strategies in the Cold: Natural Torpor and Thermogenesis*, edited by Wang L. C. H. and Hudson J. W. (Academic, New York) 1978, pp. 327–373.
[12] Lyman C. P. and O'Brien R. C., *J. Physiol. (London)*, **168** (1963) 477.
[13] Burlington R. F. and Milsom W. K., *The cardiovascular system in hibernating mammals: recent advances,* in *Living in the Cold II*, edited by Malan A. and Canguilhem B. (John Libbey Eurotext, London) 1989, pp. 235–242.
[14] Milsom W. K., Burlington R. F. and Burleson M. L., *J. Exp. Biol.*, **185** (1993) 25.
[15] Amaral L. A. N. *et al.*, *Phys. Rev. Lett.*, **86** (2001) 6026.
[16] Ivanov P. C. *et al.*, *Nature*, **399** (1999) 461.
[17] Ivanov P. C., Chen Z., Hu K. and Stanley H. E., *Physica A*, **344** (2004) 685.
[18] Ivanov P. C., Hu K., Hilton M. F., Shea S. A. and Stanley H. E., *Proc. Natl. Acad. Sci. U.S.A.*, **104** (2007) 20702.
[19] Meyer M. and Stiedl O., *Eur. J. Appl. Physiol.*, **90** (2003) 305.
[20] Meyer M. and Stiedl O., *J. Math. Biol.*, **52** (2006) 830.
[21] Meyer M., Stiedl O. and Kerman B., *Fractals*, **11** (2003) 195.
[22] Stiedl O. and Meyer M., *J. Math. Biol.*, **47** (2003) 169.
[23] Mertens A., Stiedl O., Steinlechner S. and Meyer M., *Am. J. Physiol. Regul. Integr. Comp. Physiol.*, **294** (2008) R639.
[24] Falconer F., *Fractal Geometry* (John Wiley & Sons, New York) 2003.
[25] Daoudi K., Véhel J. L. and Meyer Y., *J. Constr. Approx.*, **14** (1998) 349.
[26] Ivanov P. C., Amaral L. A. N., Goldberger A. L. and Stanley H. E., *Europhys. Lett.*, **43** (1998) 363.